Journal of Solid State Chemistry 183 (2010) 2945–2950

Contents lists available at ScienceDirect

Journal of Solid State Chemistry

journal homepage: www.elsevier.com/locate/jssc

Three 3D hybrid networks based on octamolybdates and different Cu^{I}/Cu^{II}-bis(triazole) motifs

Chun-Jing Zhang [a], Hai-Jun Pang [b], Qun Tang [a], Hui-Yuan Wang [a], Ya-Guang Chen [a,*]

[a] Key Laboratory of Polyoxometalates Science of Ministry of Education, College of Chemistry, Northeast Normal University, Changchun 130024, PR China
[b] College of Chemical and Environmental Engineering, Harbin University of Science and Technology, Harbin 150080, PR China

ARTICLE INFO

Article history:
Received 13 July 2010
Received in revised form
28 September 2010
Accepted 4 October 2010
Available online 13 October 2010

Keywords:
Organic–inorganic hybrid
Polyoxometalate
Copper
Luminescent property

ABSTRACT

Three 3D compounds based on octamolybdate clusters and various Cu^{I}/Cu^{II}-bis(triazole) motifs, $[Cu^{I}_2btb][\beta\text{-}Mo_8O_{26}]_{0.5}$ (**1**), $[Cu^{I}_2btpe][\beta\text{-}Mo_8O_{26}]_{0.5}$ (**2**), and $[Cu^{II}(btpe)_2][\beta\text{-}Mo_8O_{26}]_{0.5}$ (**3**) [btb = 1,4-bis(1,2,4-triazol-1-yl)butane, btpe = 1,5-bis(1,2,4-triazol-1-yl)pentane], were isolated via tuning flexible ligand spacer length and metal coordination preferences. In **1**, the copper(I)-btb motif is a one-dimensional (1D) chain which is further linked by hexadentate $\beta\text{-}[Mo_8O_{26}]^{4-}$ clusters via coordinating to Cu^{I} cations giving a 3D structure. In **2**, the copper(I)-btpe motif exhibits a "stairs"-like $[Cu^{I}_2btpe]^{2+}$ sheet, and the tetradentate $\beta\text{-}[Mo_8O_{26}]^{4-}$ clusters interact with two neighboring $[Cu^{I}_2btpe]^{2+}$ sheets constructing a 3D framework. In **3**, the copper(II)-btpe motif possesses a novel (2D → 3D) interdigitated structure, which is further connected by the tetradentate $\beta\text{-}[Mo_8O_{26}]^{4-}$ clusters forming a 3D framework. The thermal stability and luminescent properties of **1**–**3** are investigated in the solid state.

1. Introduction

Polyoxometalates (POMs) [1–5], as a large family of metal-oxygen clusters, constitute a fascinating class of inorganic systems with structural diversity and a wide range of applications that include, but are not limited to, catalysis [6–11], medicine [12,13], biology [14,15], and materials science [16–23]. Till date, most of the POMs have already been applied to act as building blocks to be connected with transition-metal complexes (TMCs) into POM-functional organic–inorganic hybrid materials to conflate useful properties of POMs and TMCs components, providing access to a vast area of complex, multifunctional materials [24–26].

Of the various POM structures, the octamolybdate is an interesting cluster with a variety of structural isomers, that is, α-, β-, γ-, δ-, ε-, ζ-, η-, and θ-isomer. A comprehensive investigation on these isomers has been reported by Zubieta and co-workers [27–37]. Till date, many organic–inorganic hybrids constructed from these isomers and TMCs have been synthesized. However, most of the organic components in these hybrids are rigid ligands such as *o*-phenanthroline [38–41], 2,2′-bipyridine [42–45], and 4,4′-bipyridine [46]. In comparison, the research on the introduction of TMCs with flexible ligands into hybrids based on octamolybdate clusters is comparatively scarce [47–50]. The flexible bridging ligands are regarded as a class of excellent synthons for the construction of high-dimensional hybrid solids due to their flexibility and conformation freedom. It is especially attractive that they are inclined to connect metal ions to form TMCs with coordination freedom and, further, conform to the coordination environment of POMs. Herein, we give a special study of the flexible bis(triazole) molecules, btb and btpe [btb = 1,4-bis(1,2,4-triazol-1-yl)butane, btpe = 1,5-bis(1,2,4-triazol-1-yl)pentane], with a hope to obtain informative examples for designable syntheses based on the following considerations: (i) The 1,2,4-triazole groups in ligand can provide more potential coordination sites [51–53]. (ii) The two 1,2,4-triazole rings can freely twist around the $-(CH_2)_n-$ group to meet the requirements of the coordination geometries of metal atoms in the assembly process. (iii) The $-(CH_2)_n-$ spacers in the ligands are changeable [54]. In particular, as a d^9 metal, Cu^{II} ion can be easily converted into Cu^{I} ion in the presence of different types of reducer [54–58]. The changeable oxidation states and versatile coordination geometries make copper ion a prime candidate to act as a controllable linker.

Herein, we report three 3D organic–inorganic hybrid compounds, $[Cu^{I}_2btb][\beta\text{-}Mo_8O_{26}]_{0.5}$ (**1**), $[Cu^{I}_2btpe][\beta\text{-}Mo_8O_{26}]_{0.5}$ (**2**), and $[Cu^{II}(btpe)_2][\beta\text{-}Mo_8O_{26}]_{0.5}$ (**3**) with various TMCs and final different spacial structure. Their syntheses, structures, and the luminescent properties in the solid state are presented and discussed.

2. Experimental section

2.1. Materials and general methods

All reagents were purchased commercially and were used without further purification. Elemental analyses (C, H, and N) were performed on a Perkin-Elmer 2400 CHN Elemental Analyzer.

* Corresponding author.
E-mail address: chenyg146@nenu.edu.cn (Y.-G. Chen).

0022-4596/$ - see front matter © 2010 Elsevier Inc. All rights reserved.
doi:10.1016/j.jssc.2010.10.006

IR spectra on KBr pellets were recorded on a Nicolet 170SX FT-IR spectrophotometer in the range 400–4000 cm^{-1}. TG analyses were performed with a Perkin-Elmer TGA7 instrument in an atmosphere of nitrogen at a heating rate of 10 °C min^{-1}. The X-ray powder diffraction (XRPD) patterns were recorded on a Siemens D5005 diffractometer with Cu$K\alpha$ (λ=1.5418 Å) radiation. Photoluminescence spectra were measured with pure solid sample under room temperature using a FL-2T2 instrument (SPEX, USA) with 450 W Xenon lamp monochromatized by double grating (1200).

2.2. Syntheses of 1–3

2.2.1. Synthesis of $[Cu^{I}_2btb][\beta\text{-}Mo_8O_{26}]_{0.5}$ (1)

A mixture of $Na_2MoO_4\cdot 2H_2O$ (0.2 g, 0.8 mmol), $Cu(Ac)_2\cdot H_2O$ (0.08 g, 0.4 mmol), btb (0.08 g, 0.5 mmol), and Et_3N (0.2 mL) was dissolved in 12 mL distilled water and stirred at room temperature for 30 min. The pH of the mixture was adjusted to 3.9 with 1 mol/L HCl, and then sealed in a Teflon-lined autoclave and heated at 160 °C for 4 days. After slow cooling to room temperature, red block crystals were obtained with 47% yield based on Mo. The crystals were filtered and hand-separated. Anal. calcd for $C_8H_{12}N_6Cu_2Mo_4O_{13}$ (911.10): C 10.55, H 1.33, N 9.22 (%); found: C 10.66, H 1.19, N 9.29 (%).

2.2.2. Synthesis of $[Cu^{I}_2btpe][\beta\text{-}Mo_8O_{26}]_{0.5}$ (2)

The similar synthetic procedure as that of **1** was used, except that btpe was used instead of btb. Red cuboid crystals were filtered and washed with distilled water (yield: 48% based on Mo). Anal. calcd for $C_9H_{14}Cu_2Mo_4N_6O_{13}$ (925.12): C 11.68, H 1.53, N 9.08 (%); found: C 11.56, H 1.64, N 9.17 (%).

2.2.3. Synthesis of $[Cu^{II}(btpe)_2][\beta\text{-}Mo_8O_{26}]_{0.5}$ (3)

The similar synthetic procedure as that of **2** was used, except that Et_3N was not added. Blue sheet crystals were filtered and washed with distilled water (yield: 42% based on Mo). Anal. calcd for $C_{18}H_{28}CuMo_4N_{12}O_{13}$ (1067.84): C 20.45, H 2.64, N 15.74 (%); found: C 20.36, H 2.56, N 15.61 (%).

2.3. X-ray crystallography

Single-crystal X-ray diffraction data collections of compounds **1**–**3** were performed using a Bruker Smart Apex CCD diffractometer with Mo$K\alpha$ radiation (λ=0.71073 Å) at 293 K. Multi-scan absorption corrections were applied. All the structures were solved by the directed method and refined by full-matrix least-squares on F^2 using the *SHELXTL* crystallographic software package [59,60]. The positions of hydrogen atoms on carbon atoms were calculated theoretically. A summary of the crystal data, data collection, and refinement parameters for **1**–**3** are listed in Table 1.

3. Results and discussion

The β-$[Mo_8O_{26}]^{4-}$ (shortened as β-Mo_8) anion is the inorganic building block in **1**–**3**. The β-Mo_8 anion exhibits the most compact structure of eight edge-sharing [MoO_6] octahedra with two [Mo_4O_{13}] subunits stacking together. Thus, β-Mo_8 contains fourteen terminal, six doubly bridging, four triply bridging, and two five-fold bridging oxo groups [61]. Bond valence sum calculations [62] for **1**–**3** show that all Mo atoms are in +VI oxidation state and Cu atoms are in +I oxidation state in **1** and **2** and the +II oxidation state in **3**. Additionally, the oxidation state of the Cu atoms in **1**–**3** is further confirmed by their coordination environments and crystal color. The results are consistent with the formulas of **1**–**3** given by X-ray structure determination.

Table 1
Crystal data and structure refinements for compounds **1**–**3**.

	1	2	3
Formula	$C_8H_{12}Cu_2Mo_4N_6O_{13}$	$C_9H_{14}Cu_2Mo_4N_6O_{13}$	$C_{18}H_{28}CuMo_4N_{12}O_{13}$
M	911.10	925.12	1067.84
Crystal system	Monoclinic	Monoclinic	Monoclinic
Space group	$C2/c$	$P2(1)/n$	$P2(1)/n$
a/Å	21.249(2)	11.585(1)	13.814(3)
b/Å	13.202(2)	15.389(1)	15.169(3)
c/Å	14.712(2)	11.870(2)	15.946(4)
β/°	102.573(2)	100.829(1)	96.006(3)
V/Å^3	4028.0(8)	2078.5(4)	3323.1(2)
Z	8	4	4
D_{calcd}/g cm^{-3}	3.005	2.956	2.134
T/K	293(2)	293(2)	293(2)
μ/mm^{-1}	4.568	4.429	2.174
Refl. measured	10267	10948	17371
Refl. unique	3860	3976	6359
R_{int}	0.0288	0.0375	0.0765
GoF on F^2	1.049	1.094	0.993
R_1/wR_2 [$I\geq 2\sigma(I)$]	0.0335/0.0851	0.0379/0.1027	0.0600/0.1465
R_1/wR_2 (all data)	0.0440/0.0897	0.0548/0.1169	0.1081/0.1630

$R_1=\sum||F_o|-|F_c||/\sum|F_o|$; $wR_2=\sum[w(F_o^2-F_c^2)^2]/\sum[w(F_o^2)^2]^{1/2}$.

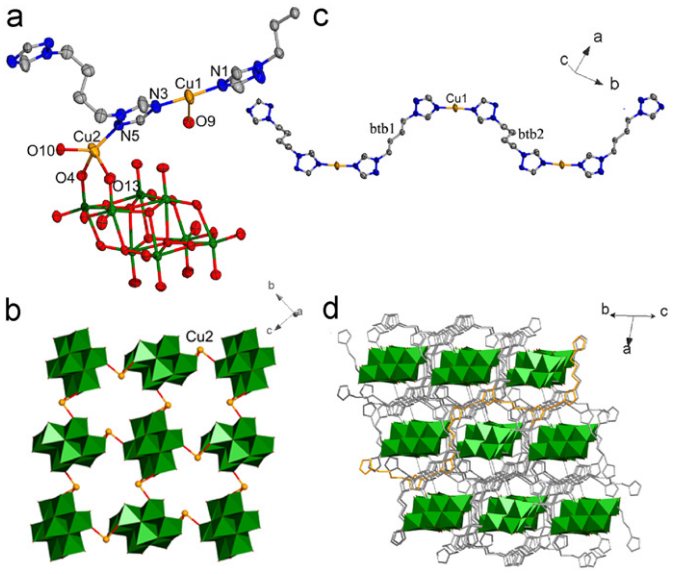

Fig. 1. (a) Coordination environment of the Cu^{I} centers in **1**. (b) Polyhedral representation of the 2D inorganic backbone in **1**. (c) View of the 1D zigzag chain in **1**. (d) Illustration of the 3D framework of **1**.

3.1. Structure description

Single-crystal X-ray diffraction analysis reveals that **1** is constructed from one β-Mo_8 anion, two kinds of Cu^{I} ions, and two kinds of btb ligands in the asymmetric unit, as shown in Fig. 1a. The $Cu^{I}(1)$ ion exhibits the [CuN_2O] T-shaped configuration, in which two nitrogen atoms come from the triazole rings of two btb groups and one oxygen atom from one β-Mo_8 anion. The bond lengths around the $Cu^{I}(1)$ are 1.879(6) and 1.877(6) Å for Cu–N bond, 2.724(4) Å for Cu–O bond. This Cu–O distance is long and is attributed to weak coordination bond according to Refs. [58,63]. $Cu^{I}(2)$ ion displays [$CuNO_3$] tetrahedral configuration which is coordinated by one nitrogen atom from the triazole ring of btb

group, three oxygen atoms from two β-Mo_8 anions. The bond lengths around the $Cu^{I}(2)$ ions are 1.929(5) Å for Cu–N bond, 1.905(4), 2.141(4), and 2.393(4) Å for Cu–O bond. Btb1 serves as a bidentate ligand connecting two $Cu^{I}(1)$ ions, while btb2 acts as a tetradentate ligand connecting two $Cu^{I}(1)$ ions and two $Cu^{I}(2)$ ions (Fig. S1). In addition, hexadentate β-Mo_8 anion bridges four $Cu^{I}(2)$ ions and two $Cu^{I}(1)$ ions (Fig. S2).

The 3D structure of **1** can be visualized in terms of a 2D inorganic subnet and a 1D metal-organic chain, connected together by sharing copper atoms. On the one hand, each β-Mo_8 anion bridges four $Cu^{I}(2)$ ions and each $Cu^{I}(2)$ ions connects two β-Mo_8 anions by three terminal oxygen atoms forming a 2D inorganic backbone (Fig. 1b). On the other band, $Cu^{I}(1)$ ions link btb1 and btb2 ligands to generate an infinite zigzag chain in ABAB type (Fig. 1c). Furthermore, each zigzag chain penetrates and connects the 2D sheet by $Cu^{I}(1)$–O9 ($Cu^{I}(1)$ from zigzag chain and O9 from 2D inorganic backbone) and $Cu^{I}(2)$–N5 ($Cu^{I}(2)$ from 2D inorganic backbones and N5 from zigzag chains) bonds into a complicated 3D structure (Fig. 1d).

Crystal structure analysis reveals that **2** consists of one β-Mo_8 anion, two Cu^{I} ions, and one btpe ligand as shown in Fig. 2a. The crystallographically unique $Cu^{I}(1)$ and $Cu^{I}(2)$ ions are both tetra-coordinated by two N atoms from two btpe ligands and two oxygen atoms from one β-Mo_8 in a "seesaw" geometry. The bond lengths around the $Cu^{I}(1)$ are 1.936(6) Å for Cu–N bond, 2.265(5) and 2.297(5) Å for Cu–O bond. The bond lengths around the $Cu^{I}(2)$ are 1.956(6) and 1.967(6) Å for Cu–N bond, 2.244(5) and 2.334(5) Å for Cu–O bond. Each Cu^{I} ion connects two btpe ligands and each btpe ligand bridges two $Cu^{I}(1)$ and two $Cu^{I}(2)$ ions to generate a "stairs"-like 2D sheet (Fig. 2b). It should be noted that the sheet contains parallelogram motif (30-membered macrocycles) with the edge distances at *ca.* 13.6 and 11.3 Å constructed from two $Cu^{I}(1)$ ions, two $Cu^{I}(2)$ ions, two btpe ligands, and two triazole of other btpe ligands. Finally, the neighboring 2D sheets are linked by the tetradentate β-Mo_8 anions via coordinating to Cu^{I} ions achieving a 3D framework (Fig. 2c).

Compound **3** is constructed from one β-Mo_8 anion, one Cu^{II} ion, and two btpe ligands as shown in Fig. 3a. There is one crystallographically independent Cu^{II} ion. The coordination sphere of $Cu^{II}(1)$ ion displays an octahedral geometry achieved by four nitrogen atoms from four btpe molecules, two terminal oxygen atom from two β-Mo_8 anions. The bond lengths around the $Cu^{II}(1)$ are 1.985(8)–2.018(8) Å for Cu–N bond, 2.501(6) and 2.515(6) Å for Cu–O bond.

An interesting structural feature is the alternating linkages between the $Cu^{II}(1)$ ion and btpe1 ligand to form left/right-helical chains along the crystallographic 2_1 screw axis in the *b* direction with a pitch of 15.17 Å (Fig. 3b). The existence of 2_1 left/right-helical chains may be because of the gauche conformation of btpe1 ligands. These opposite chirality chains are further linked together by btpe2 ligand to form a 2D $\left[Cu^{II}(btpe)_2\right]_n^{2n+}$ bilayer (Figs. 3c and S3). What deserves to be mentioned here is that the btpe2 ligands of each bilayer point into and insert the voids of the adjacent bilayers, in a mutual relationship. Finally, this unique fashion gives the novel (2D→3D) interdigitated array [64–67]. Even after the interdigitated array of identical 2D bilayers, significant void space still remains. Each β-Mo_8 anion inserts regularly in the void and connects adjacent bilayer by $Cu^{II}(1)$–O9 and $Cu^{II}(1)$–O6 covalent linkages to give rise to a 3D framework (Fig. 3d). To the best of our knowledge, compound **3** presents the first example of POM-based compound, which possesses novel interdigitated structure.

3.2. *The influencing factors on the form of compounds **1**–**3** with different 3D structures*

According to previous research, for transition metal cations, the coordination ability of the nitrogen atoms from organic ligand is stronger than the oxygen atoms of polyanion and water molecules [47,68]. Consequently, each copper cation in compounds **1**–**3** is first coordinated by nitrogen atoms from bis(triazole) ligands to form various Cu-bis(triazole) motifs. In compound **1**, the metal-organic motif is a 1D chain which is constructed by Cu^{I} ions and btb ligands. Cu^{I} ions are the reduced product from starting Cu^{II} ions by Et_3N which as an organonitrogen species can generally act as reducing agent under hydrothermal conditions and the similar trends are also observed in other polyoxometalate-based compounds [58]. In compound **2**, when the btpe ligand with $-(CH_2)_5-$ spacers is used instead of btb ligand and Cu^{I} ions are unchanged, a "stairs"-like 2D sheet is formed. By comparing compound **2** with **1**, we found that a minor change of the ligand greatly influences the structure of metal-organic motifs. This is the possible result of different conformations

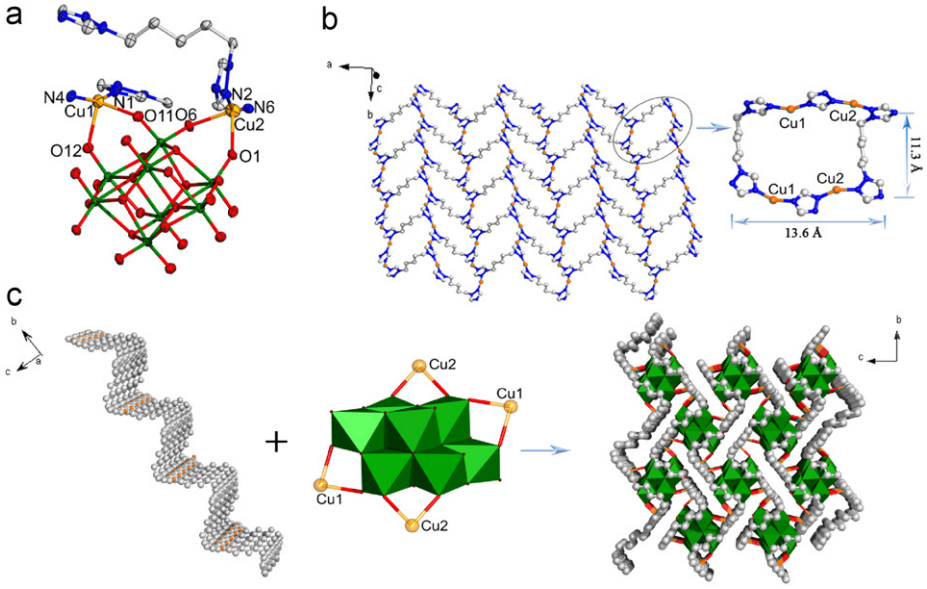

Fig. 2. (a) Coordination environment of the Cu^{I} centers in **2**. (b) View of the "stairs"-like sheet. (c) View of the 3D structure of **2** constructed from "stairs"-like sheets and ***β***-$[Mo_8O_{26}]^{4-}$ clusters.

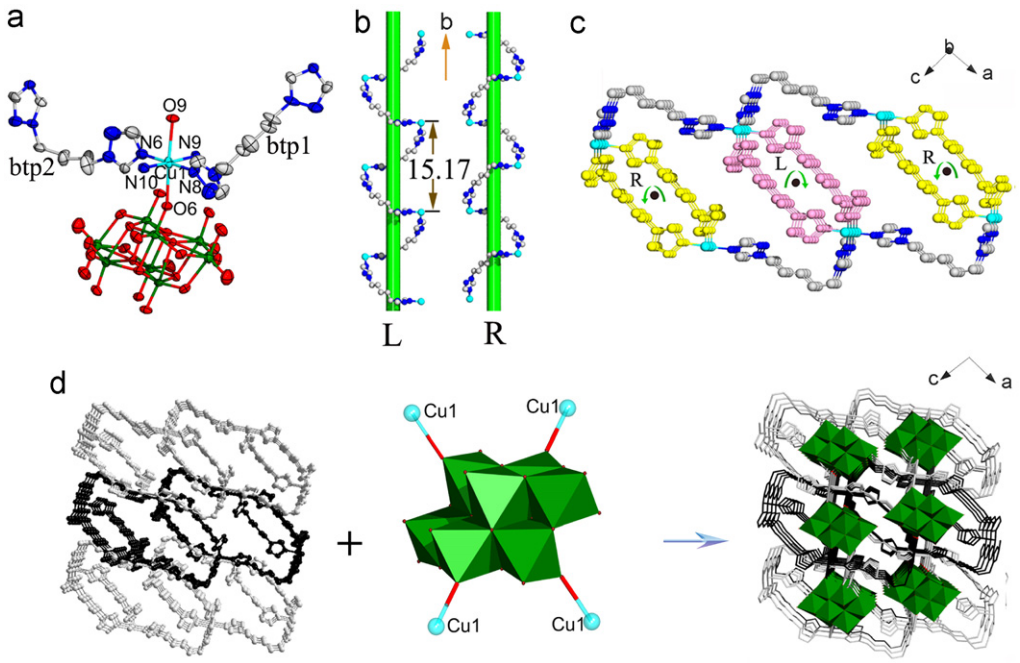

Fig. 3. (a) Coordination environment of the Cu^{II} centers in **3**. (b) Combined ball/stick representation of the left-handed (L) and right-handed (R) helical chains in **3**. (c) View of the 2D $[Cu^{II}(btpe)_2]_n^{2n+}$ bilayer. (d) View of the 3D structure of **3** constructed from (2D→3D) interdigitated structure and ***β***-$[Mo_8O_{26}]^{4-}$ clusters.

and spatial extension capacities of btb and btpe molecules. The btpe molecule with longer spacers possesses more flexible bend and free rotation when coordinating to the central metals. In compound **3**, the metal-organic motifs are 2D $[Cu^{II}(btpe)_2]_n^{2n+}$ bilayers (Fig. 3c) which mutually interdigitate, giving a novel (2D→3D) interdigitated array, when the copper ions were controlled as Cu^{II} cations and btpe ligands were still used. The obvious structural difference between metal-organic motifs in **2** and **3** may be ascribed to a higher coordination number of the Cu^{II} cation than the Cu^{I} cation. The Cu^{II} cation tends to form an elongated octahedral geometry due to the strong Jahn–Teller effect of its d^9 electronic configuration. Cu^{I} cation prefers a linear, "T-shaped", or distorted tetrahedron coordination geometry with 2–4 coordination numbers. Therefore, Cu^{II} cations are coordinated by four btpe ligands in the equatorial sites, and Cu^{I} cations are coordinated by two btpe ligands to form different copper-btpe motifs.

In summary, the length of the bis(triazole) ligands and the coordination preferences of the Cu ions implement a synergic influence on the peripheral environments of β-Mo_8 clusters and the final structures of compounds **1**–**3**. The synergic influence on the form of compounds **1**–**3** is accordant with that of the compounds constructed by Cu^{I}/Cu^{II}-bis(triazole) motifs and other polyoxometalates reported in the literatures [54,69,70].

3.3. IR spectra, XRPD patterns, and thermogravimetric analyses

The IR spectra for compounds **1**–**3** are presented in Fig. S4. The bands at 1760–1060 cm^{-1} are attributed to the triazole-ring stretching vibrations (υ(C═N)+υ(N═N)) and 3180–2830 cm^{-1} are assigned to the –CH_2– stretching vibrations in btb or btpe molecules [54]. The characteristic band at 990–475 cm^{-1} are ascribed to the υ(Mo═O) and υ(Mo–O–Mo) vibrations [43].

The XRPD patterns for compounds **1**–**3** are presented in Fig. S5. The diffraction peaks of both simulated and experimental patterns match well, indicating the phase purities of compounds **1**–**3**.

The TG analyses of **1**–**3** were performed under N_2 at a rate of 10 °C/min in the range of 25–800 °C (Fig. S6). Compound **1**–**3** are all anhydrous. In compound **1**, the weight loss of 22.0% (calc. 21.1%) from 324 to 500 °C corresponds to the loss of btb molecules. For compound **2**, the weight loss of 21.9% (calc. 22.3%) in the range of 318 – 510 °C corresponds to the loss of btpe molecules, while in compound **3**, the weight loss of btpe is 38.3% (calc. 38.8%) in the range of 296 – 777 °C. The TG analysis results of **1**–**3** supports their chemical compositions.

3.4. The luminescent properties

Recently, inorganic – organic hybrid coordination polymers, especially comprising the d^{10} metal center and aromatic containing system, been intensively investigated for attractive fluorescence properties and potential applications as new luminescent materials [71,72]. In this work, photoluminescence properties of compounds **1**–**3** were investigated in the solid state at room temperature. Compound **1** based on btb exhibits violet-fluorescent with the band at 357 nm and a shoulder band at 461 nm upon excitation at 200 nm (Fig. 4 left). Compounds **2** and **3** based on btpe display strong emission at 365 and 394 nm and weak emissions at *ca.* 460 and 458 nm, respectively, when excitation occurs at 200 nm (Fig. 4 middle and right). In order to understand the nature of the luminescence, the emission spectra of free btb and btpe were also investigated under identical experimental conditions. The free btb and btpe show strong emissions at λ_{max}=440 and λ_{max}=441 nm when excited at 378 and 382 nm, respectively (Fig. S7). In comparison with the pure btb and btpe ligand, the origin of the emission for compounds **1**–**3** can be tentatively attributable to a joint contribution of ligand-to-metal charge transfer (LMCT) (357–394 nm) and intraligand $\pi^*\rightarrow\pi$ transitions of the neutral ligand (*ca.* 460 nm) [73,74]. It is worth mentioning that the strong emission band of **3** is red-shifted as compared to that of **2**, which may be that the Cu^{II} ions can offer more advantage of energy transfer than Cu^{I} ions.

4. Conclusion

In summary, under hydrothermally synthesized reaction condition, three high-dimensional compounds based on octamolybdates

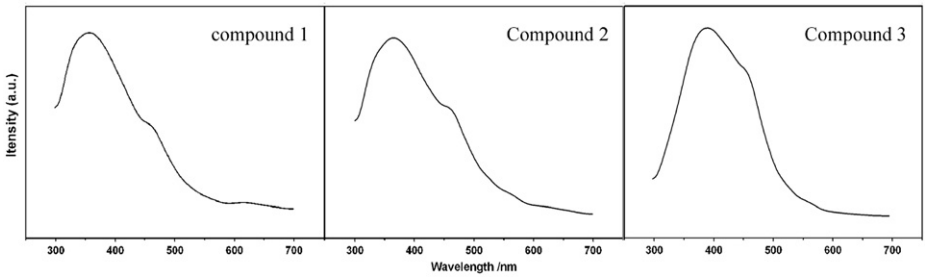

Fig. 4. Emission spectra of compounds **1**–**3** excited at 200 nm in the solid state at room temperature.

modified by different Cu^{I}/Cu^{II}-bis(triazole) motifs have been isolated. The metal-organic motif in **1** is a 1D zigzag chain, in **2** exhibits a "stairs"-like $[Cu^{I}_{2}btpe]^{2+}$ sheet, and in **3** shows a novel (2D→3D) interdigitated structure. The inorganic building block β-Mo_8 anions connect the various motifs, respectively, forming different 3D networks. The structural differences show that spacer length of flexible ligand and metal coordination preferences have great influences on the metal-organic motifs and the structure of the final assembly. The exploration of such compounds might provide an interesting model for the preparation of new high-dimensional organic–inorganic hybrids with desirable properties.

Acknowledgments

This work was supported by the analysis and testing foundation of Northeast Normal University.

Appendix A. Supporting Information

Supplementary data have been deposited with the Cambridge crystallographic center, CCDC reference numbers: 769063 for **1**, 769065 for **2**, and 769066 for **3**. Copy of this information may be obtained free of charge from The Director, CCDC, 12 Union Road, Cambridge, CB2, IEZ, UK (Fax: +44123336033; e-mail: deposit@ccdc.cam.ac.uk. Structural figures for compounds **1** and **3**, IR, XRPD, TG, luminescent spectra of free ligands btb and btpe.

Appendix B. Supporting Information

Supplementary data associated with this article can be found in the online version at doi:10.1016/j.jssc.2010.10.006.

References

[1] M.T. Pope, Heteropoly and Isopoly Oxometalates, Springer Verlag, New York, 1983.
[2] M.T. Pope, A. Müller (Eds.), Polyoxometalate Chemistry from Topology via Self-assembly to Applications, Kluwer Academic Publishers, Dordrecht, 2001.
[3] J.J. Borrys-Almener, E. Coronado, A. Müller, M.T. Pope, in: Polyoxometalate Molecular Science, Kluwer, Dordrecht, The Netherlands, 2003.
[4] A. Müller, P. Kögerler, Coord. Chem. Rev. 199 (2000) 335.
[5] D.L. Long, E. Burkholder, L. Cronin, Chem. Soc. Rev. 36 (2007) 105.
[6] V. Artero, A. Proust, P. Herson, F. Villain, C. Moulin, P. Gouzerh, J. Am. Chem. Soc. 125 (2003) 11156.
[7] C. Besson, Z.Q. Huang, Y.V. Geletii, S. Lense, K.I. Hardcastle, D.G. Musaev, T.Q. Lian, A. Proustac, C.L. Hill, Chem. Commun. 46 (2010) 2784.
[8] K. Kamata, Y. Nakagawa, K. Yamaguchi, N. Mizuno, J. Am. Chem. Soc. 130 (2008) 15304.
[9] D.B. Dang, Y. Bai, C. He, J. Wang, C.Y. Duan, J.Y. Niu, Inorg. Chem. 49 (2010) 1280.
[10] Y.H. Guo, C.W. Hu, J. Mol. Catal. A 262 (2007) 136.
[11] R.D. Gall, C.L. Hill, J.E. Walker, Chem. Mater. 8 (1996) 2523.
[12] Special Issue on Polyoxometalates, C.L. Hill (guest ed.), Chem. Rev. 98 (1998) 1.
[13] E.D. Clercq, Rev. Med. Virol. 10 (2000) 255.
[14] J.T. Rhule, C.L. Hill, D.A. Judd, Chem. Rev. 98 (1998) 327.
[15] X. Wang, J. Liu, M. Pope, Dalton Trans. (2003) 957.
[16] A. Proust, R. Thouvenot, P. Gouzerh, Chem. Commun. (2008) 1837.
[17] J. Zhang, Y.F. Song, L. Cronin, T.B. Liu, J. Am. Chem. Soc. 130 (2008) 14408.
[18] J. Zhang, J. Hao, Y.G. Wei, F.P. Xiao, P.H. Yin, L.S. Wang, J. Am. Chem. Soc. 132 (2010) 14.
[19] P. Mialane, A. Dolbecq, F. Sécheresse, Chem. Commun. (2006) 3477.
[20] B.S. Bassil, S.S. Mal, M.H. Dickman, U. Kortz, H. Oelrich, L. Walder, J. Am. Chem. Soc. 130 (2008) 6696.
[21] X. Fang, P. Kögerler, L. Isaacs, S. Uchida, N. Mizuno, J. Am. Chem. Soc. 131 (2009) 432.
[22] J.-W. Zhao, H.-P. Jia, J. Zhang, S.-T. Zheng, G.-Y. Yang, Chem. Eur. J. 13 (2007) 10030.
[23] J.Y. Niu, P.T. Ma, H.Y. Niu, J. Li, J.W. Zhao, Y. Song, J.P. Wang, Chem. Eur. J. 13 (2007) 8739.
[24] C.Y. Sun, S.X. Liu, D.D. Liang, K.Z. Shao, Y.H. Ren, Z.M. Su, J. Am. Chem. Soc. 131 (2009) 1883.
[25] L.S. Long, CrystEngComm 12 (2010) 1354.
[26] D.-L. Long, R. Tsunashima, L. Cronin, Angew. Chem. Int. Ed. 49 (2010) 1736.
[27] P.J. Hagrman, D. Hagrman, J. Zubieta, Angew. Chem. Int. Ed. 38 (1999) 2638.
[28] D. Hagrman, C. Zubieta, D.J. Rose, J. Zubieta, R.C. Haushalter, Angew. Chem. Int. Ed. 36 (1997) 873.
[29] D. Hagrman, C. Sangregorio, C.J. O'Connor, J. Zubieta, J. Chem. Soc. Dalton Trans. (1998) 3707.
[30] D.G. Allis, E. Burkholder, J. Zubieta, Polyhedron 23 (2004) 1145.
[31] D.G. Allis, R.G. Rarig Jr., E. Burkholder, J. Zubieta, J. Mol. Struct. 688 (2004) 11.
[32] D. Hagrman, P.J. Zapf, J. Zubieta, Chem. Commun. (1998) 1283.
[33] R.S. Rarig Jr., J. Zubieta, Inorg. Chim. Acta 312 (2001) 188.
[34] R.S. Rarig Jr., J. Zubieta, Polyhedron 22 (2003) 177.
[35] R.S. Rarig Jr., J. Zubieta, J. Chem. Soc. Dalton Trans. (2001) 3446.
[36] P.J. Hagrman, J. Zubieta, Inorg. Chem. 38 (1999) 4480.
[37] D. Hagrman, P. Hagrman, J. Zubieta, Inorg. Chim. Acta 300–302 (2000) 212.
[38] R.Z. Wang, J.Q. Xu, G.Y. Yang, W.M. Bu, Y.H. Xing, D.M. Li, S.Q. Liu, L. Ye, Y.G. Fan, Polyhedron 18 (1999) 2971.
[39] R.Z. Wang, J.Q. Xu, G.Y. Yang, W.M. Bu, Y.H. Xing, D.M. Li, S.Q. Liu, L. Ye, Y.G. Fan, Solid State Sci. 2 (2000) 705.
[40] D.R. Xiao, Y. Hou, E.B. Wang, S.T. Wang, Y.G. Li, L. Xu, C.W. Hu, Inorg. Chim. Acta 357 (2004) 2525.
[41] J.-Q. Xu, R.-Z. Wang, G.-Y. Yang, Y.-H. Xing, D.-M. Li, W.-M. Bu, L. Ye, Y.-G. Fan, G.-D. Yang, Y. Xing, Y.-H. Lin, H.-Q. Jia, Chem. Commun. (1999) 983.
[42] C.Y. Sun, E.B. Wang, D.R. Xiao, H.Y. An, L. Xu, J. Mol. Struct. 741 (2005) 149.
[43] W.B. Yang, C.Z. Lu, H.H. Zhuang, J. Chem. Soc. Dalton Trans. (2002) 2879.
[44] C.-M. Wang, Q.-X. Zeng, J. Zhang, Guo-Yu Yang, Z. Anorg. Allg. Chem. 631 (2005) 838.
[45] L.D. Chen, Y.H. Wang, C.W. Hu, L.Y. Feng, E.B. Wang, N.H. Hu, H.Q. Jia, J. Solid State Chem. 161 (2001) 173.
[46] H.-H. Yu, X.-B. Cui, J. Lu, Y.-H. Sun, W.-J. Duan, J.-W. Cui, Z.-H. Yi, J.-Q. Xu, T.-G. Wang, J. Mol. Struct. 879 (2008) 156.
[47] S.L. Li, Y.Q. Lan, J.F. Ma, J. Yang, X.H. Wang, Z.M. Su, Inorg. Chem. 46 (2007) 8283.
[48] Y.Q. Lan, S.L. Li, X.L. Wang, K.Z. Shao, Z.M. Su, E.B. Wang, Inorg. Chem. 47 (2008) 529.
[49] H.-Y. Zang, Y.-Q. Lan, G.-S. Yang, X.-L. Wang, K.-Z. Shao, G.-J. Xu, Z.-M. Su, CrystEngComm 12 (2010) 434.
[50] B.-X. Dong, Q. Xu, Inorg. Chem. 48 (2009) 586.
[51] U. Beckmann, S. Brooker, Coord. Chem. Rev. 245 (2003) 17.
[52] X.-L. Wang, C. Qin, E.-B. Wang, Z.-M. Su, Chem. Commun. (2007) 4245.
[53] X.F. Kuang, X.Y. Wu, R.M. Yu, J.P. Donahue, J.S. Huang, C.-Z. Lu, Nat. Chem. 2 (2010) 461.
[54] A.-X. Tian, J. Ying, J. Peng, J.-Q. Sha, Z.-G. Han, J.-F. Ma, Z.-M. Su, N.-H. Hu, H.-Q. Jia, Inorg. Chem. 47 (2008) 3274.
[55] C.D. Wu, C.Z. Lu, H.H. Zhuang, J.S. Huang, Inorg. Chem. 41 (2002) 5636.
[56] C.M. Liu, D.Q. Zhang, D.B. Zhu, Cryst. Growth Des. 5 (2005) 1639.
[57] K. Pavani, S.E. Lofland, K.V. Ramanujachary, A. Ramanan, Eur. J. Inorg. Chem. (2007) 568.
[58] Y.-Q. Lan, S.-L. Li, X.-L. Wang, K.-Z. Shao, D.-Y. Du, H.-Y. Zang, Z.-M. Su, Inorg. Chem. 47 (2008) 8179.
[59] G.M. Sheldrick, in: SHELX-97, Program for Crystal Structure Refinement, University of Göttingen, Germany, 1997.
[60] G.M. Sheldrick, in: SHELXL-97, Program for Crystal Structure Solution, University of Göttingen, Germany, 1997.

[61] S.M. Chen, C.Z. Lu, Y.Q. Yu, Q.Z. Zhang, X. He, Inorg. Chem. Commun. 7 (2004) 1041.
[62] I.D. Brown, D. Altermatt, Acta Crystallogr. Sect. B 41 (1985) 244.
[63] R.M. Yu, X.-F. Kuang, X.-Y. Wu, C.-Z. Lu, J.P. Donahue, Coord. Chem. Rev. 253 (2009) 2872.
[64] M. Eddaoudi, D.B. Moler, H. Li, B. Chen, T.M. Reineke, M. O'Keeffe, O.M. Yaghi, Acc. Chem. Res. 34 (2001) 319.
[65] M.J. Zaworotko, B. Moulton, Chem. Rev. 101 (2001) 1629.
[66] P. Ayyappa, O.R. Evans, W. Lin, Inorg. Chem. 41 (2002) 3328.
[67] X.-Long Wang, C. Qin, E.-B. Wang, L. Xu, Z.-M. Su, C.-W. Hu, Angew. Chem. Int. Ed. 43 (2004) 5036.
[68] A. Ramanan, M.S. Whittingham, Cryst. Growth Des. 6 (2006) 2419.
[69] A.-X. Tian, J. Ying, J. Peng, J.-Q. Sha, H.-J. Pang, P.-P. Zhang, Y. Chen, M. Zhu, Z.-M. Su, Inorg. Chem. 48 (2009) 100.
[70] A.-X. Tian, J. Ying, J. Peng, J.-Q. Sha, H.-J. Pang, P.-P. Zhang, Y. Chen, M. Zhu, Z.-M. Su, Cryst. Growth Des. 8 (2008) 3717.
[71] C. Seward, W.-L. Jia, R.-Y. Wang, G.D. Enright, S. Wang, Angew. Chem. Int. Ed. 43 (2004) 2933.
[72] S.V. Ganesan, S. Natarajan, Inorg. Chem. 43 (2004) 198.
[73] L.J. Chen, X. He, C.K. Xia, Q.Z. Zhang, J.T. Chen, W.B. Yang, C.Z. Lu, Cryst. Growth Des. 6 (2006) 2076.
[74] L.-Y. Zhang, G.-F. Liu, S.-L. Zheng, B.-H. Ye, X.-M. Zhang, X.-M. Chen, Eur. J. Inorg. Chem. (2003) 2965.